Image super-resolution by TV-regularization

Antonio Marquina* and Stanley J Osher†

July 5, 2007

Abstract

In this paper we formulate a new time dependent convolutional model for super-resolution based on a constrained variational model that uses the total variation of the signal as a regularizing functional. The model uses a dataset of low resolution images and incorporates a downsampling operator to relate the high resolution scale to the low resolution one. We present an algorithm for the model and we perform a series of numerical experiments to show evidence of the good behavior of the numerical scheme and quality of the results.

Key Words. Total variation restoration, blind deconvolution, Gaussian blur, denoising.

1 Introduction

A recording device or a scanner records a signal or image so that:

- the recorded intensity of a small region is related to the true intensities of a neighborhood of a pixel through a degradation process usually called blurring
- the recorded intensities are contaminated by random noise
- the acquired signal is not well resolved.

  The general image restoration problem consists in reconstructing a signal for which the previous degradation effects are removed from the acquired signal.

The super-resolution problem consists in recovering a high resolution image from low resolution degraded images.

Classical models and algorithms for solving the super-resolution problem have been mainly based on least squares, Fourier series, and other L^2-norm approximations and consequently the results are contaminated by Gibbs' phenomena (ringing) and/or smearing near edges.

We restrict our discussion to R^2 for the sake of simplicity. An image can be interpreted as either a real function defined on Ω, a bounded and open domain in R^2 or as a suitable discretization of this continuous image. Let us denote by f the observed image and u the true image we want to recover. A

*Departamento de Matematica Aplicada, Universidad de Valencia, C/ Dr Moliner, 50, 46100-Burjassot, Spain, e-mail: marquina@uv.es

†Department of Mathematics, University of California Los Angeles, Los Angeles, CA, 90095, e-mail: sjo@math.ucla.edu

model of blurring comes from the degradation of u through some kind of averaging. We will assume that the blurring operator is defined from a kernel $h(x, y) \geq 0$ as

$$(h * u)(x, y) = \int_{\Omega} u(s, r)h(x - s, y - r)dsdr \tag{1}$$

such that

$$\int_{-\infty}^{+\infty}\int_{-\infty}^{+\infty} h(s, r)dsdr = 1 \tag{2}$$

The standard model of degradation we assume is

$$h * u + n = f \tag{3}$$

where n is Gaussian white noise.

The usual approach consists in solving the following constrained variational problem

$$\begin{array}{ll} \min_u R(u) & \\ \text{subject to} & ||h * u - f||^2_{L^2} = \sigma^2 \end{array} \tag{4}$$

where σ is the standard deviation of the noise and $R(u)$ is the so-called regularizing functional that measures the quality of the image u in the sense that smaller values of $R(u)$ correspond to better images.

This problem can be solved by formulating the Tikhonov unconstrained formulation that consists in solving the variational problem

$$u = \text{argmin}\{R(u) + \frac{\lambda}{2}[||h * u - f||^2_{L^2} - \sigma^2]\} \tag{5}$$

for an specific value of the Lagrange multiplier $\lambda > 0$.

If $R(u)$ is a quadratic functional (e.g. $R(u) = ||\nabla u||^2_{L^2}$) the problem does not allow discontinuities in the solution u therefore the edges can not be satisfactorily recovered.

In [14] the total variation norm was proposed as regularizing functional for the image restoration problem

$$TV(u) = \int_{\Omega} |\nabla u| dxdy \tag{6}$$

The variational problem (5) using the functional (6) allows to recover edges of the original image avoiding ringing and removing noise ([13, 10, 17]). We will use the signal-to-noise-ratio of the image u to measure the level of noise as

$$SNR := \frac{||u - \bar{u}||_{L^2}}{||n||_{L^2}}$$

where $\bar{u}$ is the mean value of the signal u and σ is the standard deviation of the noise.

In this research work we address the super-resolution problem. The main goal of super-resolution is to maximize the spatial resolution of the image from a dataset of low resolution images without a loss in signal-to-noise ratio. The resolution of an image is determined by the physical characteristics of the imaging system: the optics, the density of the detector elements and their spatial response. The resolution improvement of the image system can be prohibitive. An increase in the sampling rate could be achieved by obtaining more samples of the imaged object.

The super-resolution problem consists in obtaining a high-resolution image from a data set of low resolution images. This restoration problem is ill conditioned since high resolution and low resolution images are typically related through a convolution operator and a down-sampling operator. Super-resolution algorithms are useful for Magnetic Resonance Imaging inter-slice reconstruction and video processing ([6, 12]). Several models have been proposed in the literature but the convolutional ones appear to be the most reasonable to get optimal results ([6]).

A variational model using the TV norm as regularizing functional for deblurring and oversampling a single noisy image was proposed in [7] (see also [8]). This model was formulated and solved in the Fourier domain assuming periodic boundary conditions by means of the gradient descent method and using characteristic functions as convolution kernels.

In this paper we present a variational model to solve the more general super-resolution problem using the TV norm as regularizing functional. The proposed model uses a multi-frame dataset instead of a single image and Gaussian kernels of convolution allowing homogeneous Neumann boundary conditions. In addition, we propose an iterative refinement procedure based on an original idea by Bregman [1], as suggested and implemented in [11], to improve spatial resolution. We formulate an explicit algorithm to approximate the solution to this model. A set of numerical experiments is presented to show evidence of the good behavior of the model. The algorithm recovers well edges, reduces noise and captures some small features not appearing in the low resolution images.

The paper is organized as follows: in section 2 we present the new model, section 3 contains the Bregman iterative refinement procedure applied to the original model, section 4 is devoted to the algorithm and the implementation details and section 5 contains the numerical experiments.

2 A super-resolution convolutional model based on TV regularization

Let Ω_L be a subset of $\Omega \subset \mathbb{R}^2$. We define a low resolution image f as a real function defined in Ω_L. We assume that high resolution images are those whose domain is Ω. We consider a down-sampling linear operator D acting on high resolution images with values in low resolution ones . Let S be its transpose.

Given a low resolution image f the one frame model of super-resolution we assume is

$$f = D(h * u) + n \tag{7}$$

where u the unknown high resolution image, h is a given translation invariant convolution kernel and n is Gaussian white noise with zero mean and variance σ^2.

The kernel h is determined as the PSF of the sensor. The kernel could be another unknown of the problem (blind deconvolution) and in this case it is supposed to be Gaussian,

$$h(x, y) := \frac{1}{4\pi\alpha} e^{-(x^2+y^2)/4\alpha} \tag{8}$$

We can state the unconstrained variational problem using the TV-norm as regularizing functional as follows:

$$u = \text{argmin}\{TV(u) + \frac{\lambda}{2}[||f - D(h * u)||_{L^2}^2 - \sigma^2]\} \tag{9}$$

Multiframe model: Given N low resolution images, f_k, $k = 1, 2, \cdots, N$, the convolutional model describing the relation between u and f_k is expressed by a set of linear equations

$$f_k = D_k(h * u) + n_k \qquad k = 1, \cdots, N \tag{10}$$

where D_k is a down-sampling operator and n_k is Gaussian white noise with zero mean and variance σ_k^2.

In this case we can formulate the multi-frame model for super-resolution as

$$u = \arg\min_u \left\{ \int |\nabla u| + \sum_{k=1}^{N} \frac{\lambda_k}{2} \left[||f_k - D_k(h * u)||_{L^2}^2 - \sigma_k^2 \right] \right\} \tag{11}$$

where $\lambda_k > 0$ are the Lagrange multipliers weighting the constraints.

The Euler-Lagrange equations associated to this variational problem is

$$\nabla \frac{\nabla u}{|\nabla u|} + \sum_{k=1}^{N} \lambda_k (\tilde{h} * S_k(f_k) - \tilde{h} * (S_k \circ D_k(h * u)) = 0 \tag{12}$$

where S_k is the transposed operator ("up-sampling") to D_k and $\tilde{h}$ is the transpose of h.

We can re-write the Euler-Lagrange equation (12) as

$$\nabla \frac{\nabla u}{|\nabla u|} + \lambda \tilde{h} * (\bar{g} - T(h * u)) = 0 \tag{13}$$

where $\lambda = \sum_{k=1}^{N} \lambda_k$, $\bar{g} = \sum_{k=1}^{N} \frac{\lambda_k}{\lambda} S_k(f_k)$ and the operator $T := \sum_{k=1}^{N} \frac{\lambda_k}{\lambda} S_k \circ D_k$.

If $D_k = D$ is the same operator for all k then the operator $T = S \circ D$ and $\bar{g} = S(\sum_{k=1}^{N} \frac{\lambda_k}{\lambda} f_k)$ where S is the transposed of D.

In order to reduce the parameter fitting of the $\lambda_k's$ we will assume a fixed averaging procedure, (e.g. $\lambda_k := \frac{\lambda}{N}$, $k = 1, 2, \cdots, N$) to compute $\bar{g}$ and T and therefore λ will be the only parameter to be estimated.

We can solve the Euler-Lagrange equation (13) by means of the gradient-descent method formulated as the time evolution equation

$$u_t = \nabla \frac{\nabla u}{|\nabla u|} + \lambda \tilde{h} * (\bar{g} - T(h * u)) \tag{14}$$

with homogeneous Neumann boundary conditions and initiating with

$$u_0 := \frac{1}{N} \sum_{k=1}^{N} S_k(f_k) \tag{15}$$

We have tested different averaging procedures apart from the arithmetic mean. The following average has been shown a good choice

$$\frac{\lambda_k}{\lambda} = \frac{TV(f_k)}{\sum_{k=1}^{N} TV(f_k)} \tag{16}$$

If $f_0 := \frac{1}{N} \sum_{k=1}^{N} f_k$ the SNR of f_0 will be larger than the SNR of each of the f_k signals. Thus, the noise of f_0 is reduced due to the averaging.

To analyze precisely the convenience of using more than one degraded image as initial data we consider the particular case of the deconvolution problem from a set of degraded images using the variational model (11) and taking the down-sampling operators equal to the identity and the quadratic norm as regularizing functional

$$||u||^2 = \int_\Omega |\nabla u|^2. \tag{17}$$

The Euler-Lagrange equation associated to the problem

$$u = \arg\min_u \left\{ \int |\nabla u|^2 + \frac{\lambda}{2}\frac{1}{N}\sum_{k=1}^{N} ||f_k - h * u||_{L^2}^2 \right\} \tag{18}$$

using $\lambda_k = \frac{\lambda}{N}$ for all k, will be

$$\Delta u + \lambda \tilde{h} * [f_0 - h * u] = 0 \tag{19}$$

with homogeneous Neumann boundary conditions and $f_0 := \frac{1}{N}\sum_{k=1}^{N} f_k$

Applying Fourier transform to equation (19) preserving the imposed boundary conditions ("cosine transform") the following equation is obtained in the frequency domain

$$-\frac{1}{(j^2+l^2)}\hat{u}(j,l) + \lambda\hat{\tilde{h}}(j,l)\hat{f}_0 - \lambda\hat{\tilde{h}}(j,l)\hat{h}(j,l)\hat{u}(j,l) = 0 \tag{20}$$

from where we obtain

$$\hat{u}(j,l) = \frac{\lambda\hat{\tilde{h}}(j,l)\hat{f}_0(j,l)}{\frac{1}{j^2+l^2} + \lambda|\hat{\tilde{h}}(j,l)|^2} \tag{21}$$

with $\hat{f}_0(j,l) = \frac{1}{N}\sum_{k=1}^{N}\hat{f}_k(j,l)$

High frequencies of f_k are contaminated by noise. The average process allows to reduce the amplitude of high frequencies in the f_0 signal. Hence, equation (21) allows to recover more frequencies of u as N the number of images increase.

3 Bregman iteration and inverse scale space method

Since we want to recover finer scales the Bregman iterative refinement is suitable for this purpose, see [11].

The Bregman iterative refinement applied to equation (13) reads as follows: if u_0 is the solution of equation (13)

$$\nabla\frac{\nabla u_0}{|\nabla u_0|} + \lambda\tilde{h} * (\bar{g} - T(h * u_0)) = 0 \tag{22}$$

we denote v_0 the residual calculated in the high resolution scale, ie,

$$v_0 = \bar{g} - T(h * u_0) \tag{23}$$

Then we solve again the Euler-Lagrange equation for the signal $\bar{g} + v_0$ and the solution u_1 will satisfy

$$\nabla\frac{\nabla u_1}{|\nabla u_1|} + \lambda\tilde{h} * \Big(\bar{g} + v_0 - T(h * u_1)\Big) = 0 \tag{24}$$

and the new residual is defined as

$$v_1 = \bar{g} + v_0 - T(h * u_1) \tag{25}$$

and so on. Thus the sequence of Bregman iterates $u_0, u_1, \cdots, u_i, \cdots$ is obtained.

This procedure first recovers fine scales of the image and then recovers the noise. For this reason this procedure must be stopped when the quality of the obtained image is satisfactory.

This discrete process can be done more precisely by a continuum process that depends on a temporal variable acting as a scale variable. These methods are called inverse scale space methods and were introduced for variational problems with quadratic regularizing functional in [15] and for TV-restoration models in [2]. In [9] these methods have been used for image blind deconvolution based on total variation. An inverse scale space method consists of a time evolution equation that begins with signal $u_0 = 0$ and evolves to the restored image in a way such that the coarser scales converge faster than finer ones. The restored image corresponds to the one with minimum time for which the L^2-norm of the residual is approximately the standard deviation of the noise ([9]).

We propose a new nonlinear inverse scale space method to solve the super-resolution problem based on the variational problem (11) as follows:

$$u_t = \nabla \frac{\nabla u}{|\nabla u|} + \lambda \Big[\tilde{h} * \Big(\bar{g} - T(h * u) \Big) + v \Big] \tag{26}$$

$$v_t = \alpha \tilde{h} * \Big(\bar{g} - T(h * u) \Big) \tag{27}$$

where $u|_{t=0} = v|_{t=0} = 0$ and $\lambda > 0$, $\alpha > 0$ are constants.

The restored image is the one obtained for the minimum time for which

$$||f_k - d_k(h * u)||_L^2 \approx \sigma_k, \qquad k = 1, 2, \cdots, N \tag{28}$$

where σ_k is the standard deviation of the noise of f_k.

If $\hat{h}$ is the Fourier transform of h, the parameter α has to satisfy

$$0 < \alpha \leq \frac{\lambda}{4} |\hat{h}|^2$$

as demonstrated in [9].

If the kernel h is not given, h is assumed to be a Gaussian kernel.

4 An explicit numerical scheme

The Euler-Lagrange derivative of the TV-norm is not well defined at points where $\nabla u = 0$, due to the presence of the term $\frac{1}{|\nabla u|}$. Then, it is common to slightly perturb the TV functional to become

$$\int_\Omega \sqrt{|\nabla u|^2 + \epsilon}\, dxdy \tag{29}$$

where ϵ is a small positive parameter or

$$\int_\Omega |\nabla u|_\epsilon dxdy \tag{30}$$

with the notation

$$|v| = \sqrt{|v|^2 + \epsilon} \tag{31}$$

for $v \in R^2$.

We can express the 2D model (14) in terms of explicit partial derivatives

$$u_t = \lambda \tilde{h} * (\bar{g} - T(h * u)) + \frac{u_{xx}(u_y^2 + \epsilon) - 2u_{xy}u_x u_y + u_{yy}(u_x^2 + \epsilon)}{(u_x^2 + u_y^2 + \epsilon)^{\frac{3}{2}}} \tag{32}$$

using u_0 from (15) as initial guess and homogeneous Neumann boundary conditions (i.e. absorbing boundary). In our experiments we will use the TV-average of the up-sampled frames.

Next we construct an explicit discrete scheme to solve (32). Consider the domain $\Omega = [0,1] \times [0,1]$. Let m be a positive integer. We define the high resolution grid as follows: we set $h = \frac{1}{2m}$, $x_i = ih$, $y_j = jh$, $i, j = 1, 2, \cdots, 2m$. The low resolution grid is defined as $x'_i = 2ih$, $y'_j = 2jh$, $i, j = 1, 2, \cdots, m$. We denote the time stepsize by Δt, and $t_n = n\Delta$ is the time discretization. Let u_{ij}^n be the approximation to the mean value of $u(x, y, t_n)$ in the computational cell

$$\left]x_i - \frac{h}{2}, x_i + \frac{h}{2}\right[\times \left]y_i - \frac{h}{2}, y_i + \frac{h}{2}\right[\tag{33}$$

i.e.

$$u_{ij}^n \approx \frac{1}{h^2} \int_{x_i - \frac{h}{2}}^{x_i + \frac{h}{2}} \int_{y_i - \frac{h}{2}}^{y_i + \frac{h}{2}} u(x, y, t_n)\,dxdy, \qquad i = 1, \cdots, 2m \qquad j = 1, \cdots, 2m \tag{34}$$

Our first order scheme reads as follows:

$$\frac{u_{ij}^{n+1} - u_{ij}^n}{\Delta t} = \lambda[\tilde{h} * (\bar{g} - T(h * u^n))]_{ij} + \left[\frac{u_{xx}^n((u_y^n)^2 + \epsilon) - 2u_{xy}^n u_x^n u_y^n + u_{yy}^n((u_x^n)^2 + \epsilon)}{[(u_x^n)^2 + (u_y^n)^2 + \epsilon]^{\frac{3}{2}}}\right]_{ij} \tag{35}$$

where operations in the term containing derivatives are understood component-wise.

Some remarks are in order concerning how to compute the right hand side of (35): we denote by $\Delta_\pm^x u_{i,j}^n := \pm(u_{i\pm1,j}^n - u_{i,j}^n)$ and $\Delta_\pm^y u_{i,j}^n := \pm(u_{i,j\pm1}^n - u_{i,j}^n)$. Then we have the following formulas to compute the term containing derivatives

$$\begin{aligned}
[u_{xx}^n]_{ij} &:= \Delta_+^x \Delta_-^x u_{ij}^n / h^2 \\
[u_{yy}^n]_{ij} &:= \Delta_+^y \Delta_-^y u_{ij}^n / h^2 \\
[u_{xy}^n]_{ij} &:= (\Delta_-^x + \Delta_+^x)(\Delta_-^y + \Delta_+^y) u_{ij}^n / 4h^2 \\
[u_x^n]_{ij} &:= (\Delta_-^x + \Delta_+^x) u_{ij}^n / 2h \\
[u_y^n]_{ij} &:= (\Delta_-^y + \Delta_+^y) u_{ij}^n / 2h
\end{aligned} \tag{36}$$

These formulas are computed at the boundaries using “mirror extension” of values to ensure homogeneous Neumann boundary conditions.

The convolutions appearing in the constraint term are computed on the high resolution grid ($2m \times 2m$) using the discrete cosine transform (DCT) to enforce the homogeneous Neumann boundary conditions, (see [3, 5]).

In this paper we will use only one down-sampling operator D for all the frames f_k so that $\bar{g} = S(\sum_{k=1}^N \frac{\lambda_k}{\lambda} f_k)$ and $T = S \circ D$. A discussion on the most convenient down-sampling operator sampling to be used is out of the scope of this paper, (see [16, 4]).

The one dimensional down-sampling operator D^x acting on vectors $(e_i) \in R^{2m}$ with values in R^m is defined as the $m \times 2m$ matrix

$$D^x = \frac{1}{\sqrt{2}} \begin{bmatrix} 1 & 1 & 0 & 0 & \dots & 0 & 0 \\ 0 & 0 & 1 & 1 & \dots & 0 & 0 \\ \vdots & \vdots & \vdots & \vdots & \ddots & \vdots & \vdots \\ 0 & 0 & 0 & 0 & \dots & 1 & 1 \end{bmatrix}$$

and $D^x(e) := \frac{1}{\sqrt{2}}(e_1 + e_2, e_3 + e_4, \cdots, e_{2m-1} + e_{2m}) \in R^m$

The one-dimensional transposed $S^x : R^m \to R^{2m}$, $c \in R^m$ is the $2m \times m$ matrix, $S^x(c) = \frac{1}{\sqrt{2}}(c_1, c_1, c_2, c_2, \cdots, c_m, c_m)$.

Let $u = (u_{ij}) \in R^{2m} \times R^{2m}$ and $f = (f_{ij}) \in R^m \times R^m$. The two-dimensional down-sampling operator is defined as

$$f = D(u) := D^x \cdot u \cdot S^x \tag{37}$$

where the righthand side operations are understood as matrix multiplications.

The transposed operator S is defined as

$$u = S(f) := S^x \cdot f \cdot D^x \tag{38}$$

It is easy to see that $D \circ S = I_{m \times m}$ ($m \times m$ identity matrix) and $T = S \circ D \neq I_{2m \times 2m}$, therefore the up-sampling operator is reversible and the down sampling one is not.

We can write the explicit expressions of the operators for $m = 2$

$$D \begin{bmatrix} u_{11} & u_{12} & u_{13} & u_{14} \\ u_{21} & u_{22} & u_{23} & u_{24} \\ u_{31} & u_{32} & u_{33} & u_{34} \\ u_{41} & u_{42} & u_{43} & u_{44} \end{bmatrix} = \frac{1}{2} \begin{bmatrix} u_{11} + u_{12} + u_{21} + u_{22} & u_{13} + u_{14} + u_{23} + u_{24} \\ u_{31} + u_{32} + u_{41} + u_{42} & u_{33} + u_{34} + u_{43} + u_{44} \end{bmatrix}$$

$$S \begin{bmatrix} f_{11} & f_{12} \\ f_{21} & f_{22} \end{bmatrix} = \frac{1}{2} \begin{bmatrix} f_{11} & f_{11} & f_{12} & f_{12} \\ f_{11} & f_{11} & f_{12} & f_{12} \\ f_{21} & f_{21} & f_{22} & f_{22} \\ f_{21} & f_{21} & f_{22} & f_{22} \end{bmatrix}$$

$$(S \circ D) \begin{bmatrix} u_{11} & u_{12} & u_{13} & u_{14} \\ u_{21} & u_{22} & u_{23} & u_{24} \\ u_{31} & u_{32} & u_{33} & u_{34} \\ u_{41} & u_{42} & u_{43} & u_{44} \end{bmatrix} =$$

$$\frac{1}{4} \begin{bmatrix} u_{11} + u_{12} + u_{21} + u_{22} & u_{11} + u_{12} + u_{21} + u_{22} & u_{13} + u_{14} + u_{23} + u_{24} & u_{13} + u_{14} + u_{23} + u_{24} \\ u_{11} + u_{12} + u_{21} + u_{22} & u_{11} + u_{12} + u_{21} + u_{22} & u_{13} + u_{14} + u_{23} + u_{24} & u_{13} + u_{14} + u_{23} + u_{24} \\ u_{31} + u_{32} + u_{41} + u_{42} & u_{31} + u_{32} + u_{41} + u_{42} & u_{33} + u_{34} + u_{43} + u_{44} & u_{33} + u_{34} + u_{43} + u_{44} \\ u_{31} + u_{32} + u_{41} + u_{42} & u_{31} + u_{32} + u_{41} + u_{42} & u_{33} + u_{34} + u_{43} + u_{44} & u_{33} + u_{34} + u_{43} + u_{44} \end{bmatrix}$$

5 Numerical results

In this section some numerical examples are presented to illustrate the good behavior of the model and efficiency of the proposed algorithm. The results indicate that the algorithm recovers well edges and small features not appearing in the original degraded dataset without loss in the signal to noise ratio.

All our calculations are performed using a CFL restriction on the time stepsize of the form

$$\frac{\Delta t}{h^2} \leq 0.1 \tag{39}$$

We have chosen a Lagrange multiplier λ near the largest one for which the scheme is stable. We have used the value $\epsilon = 1e-4$ for the regularization of the total variation functional. The low resolution degraded images used are 128×128 pixels of resolution and dynamic range in $[0, 255]$. The results obtained are 256×256 pixels of resolution.

5.1 Example

In this example we test our model using a data set of 10 synthetic images of 128×128 pixels from the original 256×256 image (Figure 1) generated as follows. We consider a 129×129 discrete approximation of a Gaussian kernel h (Figure 1) defined from (8) setting $\alpha = 10$. We convolve the original image with the kernel and we add 10 different Gaussian white noise with SNR$\approx$ 10 to generate 10 degraded frames of 256×256. Then we apply the down-sampling operator D to obtain the 10 128×128 low resolved and degraded frames. In Figure 2 we display one of the frames of this data set (left picture) and the up-sampled and averaged image (right picture).

We apply our algorithm using $\lambda = 20$ and CFL$= 0.1$, by using equation (35) and performing 400 iterations. The result is shown in Figure 3. We observe that edges are recovered well.

In order to improve spatial resolution we apply the Bregman iterative refinement procedure using the same parameters and number of iterations as in the original model and we display the first and second Bregman iterates in Figure 4, left and right, respectively. We observe a better resolution in the restored Bregman iterates.

To show numerical evidence that super-resolving an image from several low resolution images is better than from only one we have tested our algorithm using just one frame (Figure 2, left). The result is displayed in Figure 5 where we observe more noise and a less resolved image.

Acknowledgments

Research supported by Spanish grant DGICYT MTM2005-07708 and NSF grants DMS-0312222, ACI-0321917 and NIH G54 RR021813.

References

[1] L. Bregman, The Relaxation Method of Finding the Common Points of Convex Sets and its Application to the Solution of Problems in Convex Programming, in *U.S.S.R. Comput. Math. and Math. Phys.*, 7(1967), pp. 200-217.

[2] M. Burger, G. Gilboa, S. Osher and J. Xu. Nonlinear inverse scale space methods in *Communications in Mathematical Sciences* Vol 4, No.1, pp. 179-212, 2006.

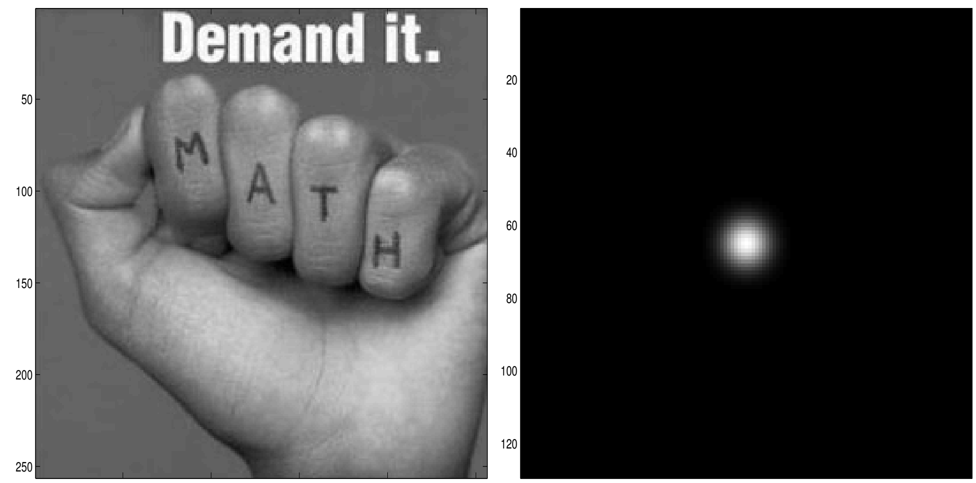

Figure 1: Left, original 256×256 image. Right, PSF 129×129

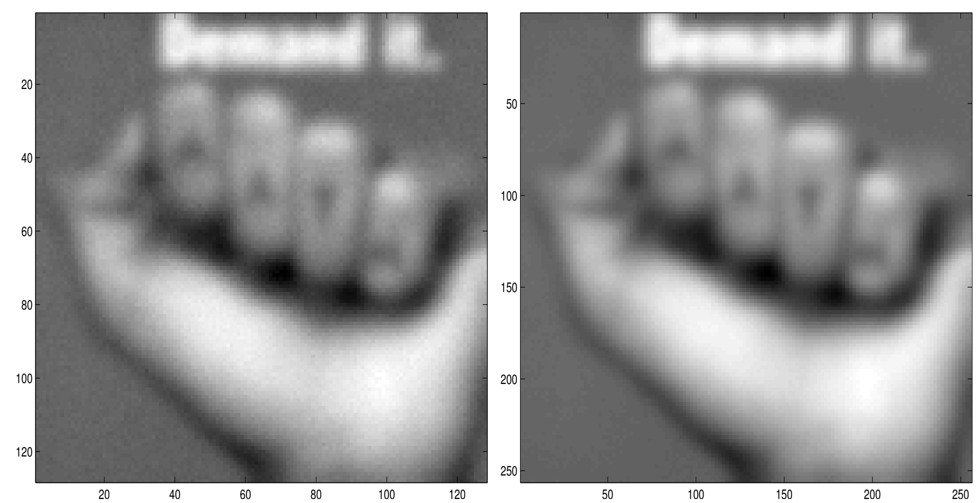

Figure 2: Left, 128×128 low resolution degraded frame. Right, up-sampled and averaged image

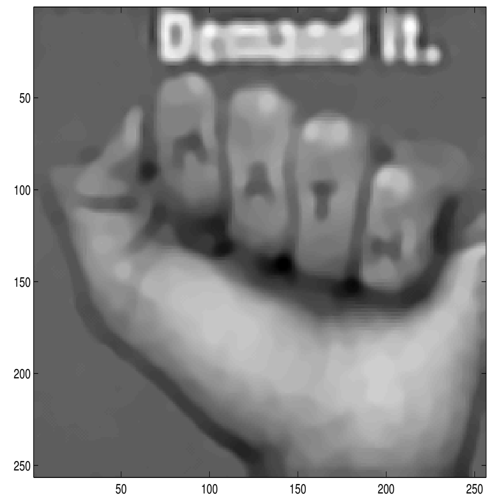

Figure 3: 256×256 super-resolved image

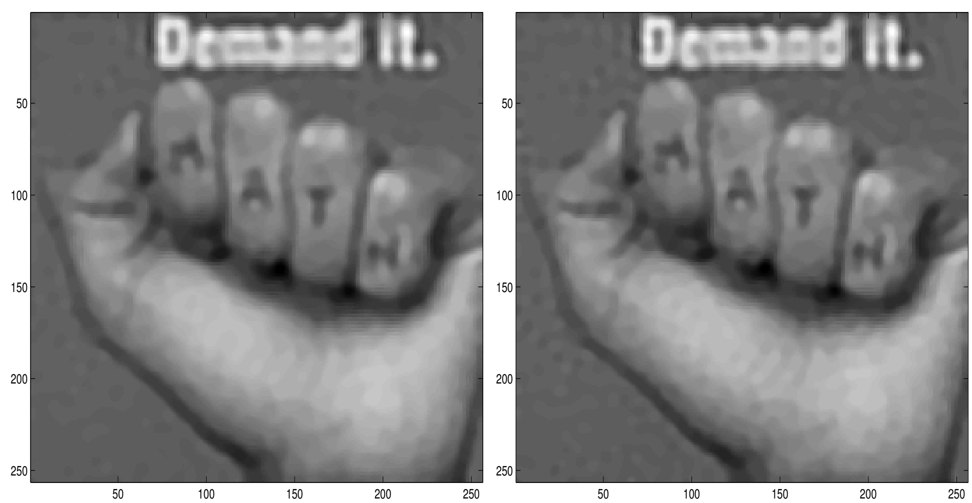

Figure 4: Left, first Bregman iteration. Right, second Bregman iteration

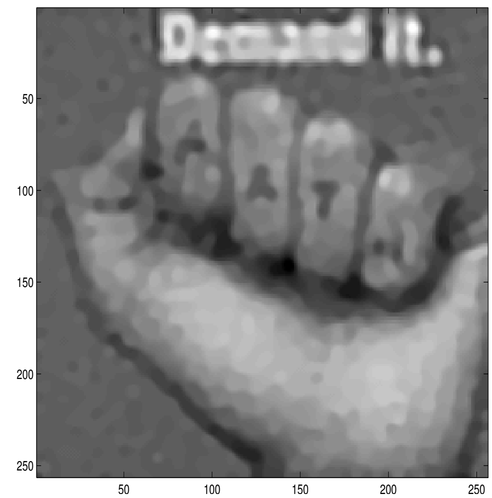

Figure 5: Solution obtained by using one frame

[3] V.F. Candela, A. Marquina and S. Serna A Local Spectral Inversion of a Linearized TV Model for Denoising and Deblurring in *IEEE Transactions on Image Processing*, Vol. 12, No 7, pp 808-816, July 2003.

[4] R.A. Gopinath and C.S. Burrus On upsampling, downsampling and rational sampling rate filter banks, in IEEE Transactions on Signal Processing, vol 42, 812-824, (1994).

[5] L. He, A. Marquina and S.J. Osher Blind deconvolution using TV regularization and Bregman iteration, in *International Journal of Imaging Systems and Technology*, 15, pp 74–83 (2005).

[6] M. Irani and S. Peleg Motion analysis for image enhancement: resolution, occlusion and transparency, in Journal of Visual Communication and Image Representation, vol 4, 324-335 (1993).

[7] F. Malgouyres, Total Variation Based oversampling of noisy images. Lecture notes in Computer Science, 2106, pp 111-122, 2001

[8] F. Malgouyres, F. Guichard, Edge direction preserving image zooming: a mathematical and numerical analysisis, SIAM J. Num. Anal.,39, pp 1-37, 2001

[9] A. Marquina, Inverse scale space methods for blind deconvolution. UCLA CAM report 06-36, 2006

[10] A. Marquina and S. Osher, Explicit Algorithms for a New Time Dependent Model Based on Level Set Motion for Nonlinear Deblurring and Noise Removal in *SIAM J. Sci. Comput.* Vol 22, No 2, pp. 387-405, 2000.

[11] S.J. Osher, M. Burger, D. Goldfarb, J. Xu and W. Jin An Iterative regularization method for total variation based image restoration *Multiscale Model and Simul.*, 4, pp.460-489, 2005.

[12] RR Peeters, P Kornprobst, M Nikolova, S. Sumert, T. Vieville, G. Malandain, R. Derich, O. Faugeras, M. Ng, P. Van Hecke, The use of super-resolution techniques to reduce slice thickness in functional MRI International Journal of Imaging Systems and Technology, vol 14, 131-138, 2004

[13] L. Rudin, S.J. Osher, Total Variation based Image Restoration with Free Local Constraints. in *Proc. of the IEEE ICIP-94*, vol. 1, Austin, TXm pp 31-35, 1994

[14] L.I. Rudin, S. Osher and E. Fatemi, Nonlinear Total Variation Based Noise Removal Algorithms in *Physica D*, 60, pp. 259-268, 1992.

[15] O. Scherzer and C. Groetsch. Inverse scale space theory for inverse problems in *Scale-Space and Morphology in Computer Vision*, M. Kerckhove, editor *Lecture Notes in Computer Science*, 2106, pp.317-325, Springer, New York, 2001.

[16] M. Unser,A. Aldrouli and M. Eden. Enlargement or reduction of digital image with minimum loss of information. IEEE Transac. on Image Processing, v4, pp 247-258 (1995).

[17] C.R. Vogel and M.E. Oman, Fast, Robust Total Variation-Based Reconstruction of Noisy, Blurred Images in *IEEE Transaction on Image Processing*, Vol 7, No 6, pp 813-824 June 1998.